Published in final edited form as:
Circ Res. 2010 May 14; 106(9): 1524–1532. doi:10.1161/CIRCRESAHA.109.212639.

Manipulation of Death Pathways in Desmin Related Cardiomyopathy

Alina Maloyan[1], **Jennifer Sayegh**[1], **Hanna Osinska**[1], **Balvin H.L. Chua**[2], and **Jeffrey Robbins**[1,*]

[1] Molecular Cardiovascular Biology, Heart Institute, Cincinnati Children's Hospital, Cincinnati, Ohio

[2] Department of Geriatrics, East Tennessee State University, Johnson City, TN

Abstract

Rationale—Transgenic mice with cardiac specific overexpression of mutated αB-crystallin ($CryAB^{R120G}$) display Desmin Related Myopathy (DRM) with dilated cardiomyopathy and heart failure. Our previous studies showed the presence of progressive mitochondrial abnormalities and activation of apoptotic cell death in $CryAB^{R120G}$ transgenic hearts. However, the role of mitochondrial dysfunction and apoptosis in the overall course of the disease was unclear.

Objective—We tested the hypothesis that prevention of apoptosis would ameliorate $CryAB^{R120G}$ pathology and decrease morbidity.

Methods and Results—We crossed $CryAB^{R120G}$ mice to transgenic mice with cardiac specific overexpression of Bcl-2. Sustained Bcl-2 overexpression in $CryAB^{R120G}$ hearts prolonged $CryAB^{R120G}$ transgenic mice survival by 20%. This was associated with decreased mitochondrial abnormalities, restoration of cardiac function, prevention of cardiac hypertrophy, and attenuation of apoptosis. $CryAB^{R120G}$ misfolded protein aggregation was significantly reduced in the double transgenic. However, inhibition of apoptotic signaling resulted in the upregulation of autophagy and alternative death pathways, the net result being increased necrosis.

Conclusion—While Bcl-2 overexpression prolonged life in this DRM model, in the absence of apoptosis, another death pathway was activated.

Keywords

heart disease; mitochondria; apoptosis; protein misfolding; autophagy; necrosis

Introduction

The R120G mutation in αB-crystallin ($CryAB^{R120G}$) causes Desmin Related Myopathy (DRM).[1] A mouse model of DRM, created by cardiomyocyte-specific overexpression of $CryAB^{R120G}$, develops progressive dilated cardiomyopathy followed by a transition to heart failure (HF).[2] We have previously shown that this model of DRM is characterized by early mitochondrial dysfunction and activation of intrinsic (mitochondrial-based) apoptotic signaling.3 While apoptotic cell death can directly cause HF,4 the sufficiency of apoptosis for

*Corresponding author: Jeffrey Robbins, MLC 7020, 240 Albert Sabin Way, Cincinnati, OH, 45229-3039. jeff.robbins@cchmc.org. Phone: 513-636-8098. Fax: 513-636-5958.

Disclosures
None

DRM-mediated HF specifically, and in protein-conformation based heart disease in general has not been explored.

The intrinsic pathway of apoptosis is regulated by the Bcl-2 family,[5] with Bcl-2 being the anti-apoptotic founding member.[6] Complex interactions between Bcl-2 family members, such as Bak and Bax can result in permeabilization of the mitochondrial outer membrane.[7] Together with MPTP opening, these two processes appear to be a general and, in most cases, terminal commitment step for the decision between cell life and death.[8] It is still unclear as to how Bcl-2 protects cells from apoptotic death. Recent studies in experimental animal models demonstrated that overexpression of Bcl-2 prevents apoptosis and injury of cardiomyocytes in post-ischemia and reperfusion hearts.[9,10] In addition, high levels of Bcl-2 were sufficient to prevent mitochondrial and contractile dysfunction in desmin null mice.[11] Apart from its anti-apoptotic function, Bcl-2 also regulates release of Ca^{2+} from the endoplasmic reticulum and reduces mitochondrial Ca^{2+} uptake.[12,13]

We wished to define the role of apoptosis in DRM pathology and determine the effects of blocking the intrinsic apoptotic pathway in terms of impacting on DRM. By crossing the $CryAB^{R120G}$ mice with transgenic (TG) mice harboring cardiac restricted overexpression of Bcl-2,[9] we asked if Bcl-2 overexpression could decrease or abolish apoptosis in the $CryAB^{R120G}$ cardiomyocytes and if inhibition of apoptosis was sufficient to prevent HF. We found that, in addition to preventing mitochondrial swelling, Bcl-2 overexpression resulted in the upregulation of autophagy, which in turn led to increased elimination of misfolded protein aggregates and a reduction in their overall accumulation. Cardiac-restricted overexpression of Bcl-2 in the $CryAB^{R120G}$ mice attenuated cardiomyocyte apoptosis by blocking the intrinsic cell death pathway, but did not prevent their ultimate death as the death process shifted towards necrosis.

Materials and Methods

Transgenic Mice

$CryAB^{R120G}$ mice and Bcl-2 overexpressing mice were used as described previously,[2,9] except that the Bcl-2 TG mice were first was bred into the FVB/N background by backcrossing the original Bcl-2 TGs to FVB/N animals for at least 7 generations. Three experimental groups were studied: single $CryAB^{R120G}$, Bcl-2 overexpressing double TG $CryAB^{R120G}$/Bcl-2, and age matched non-transgenic (NTG) littermates. TG and double TG mice were identified by PCR analysis of genomic DNA isolated from tail clips. Animals were housed in an AAALAC-approved facility and experiments were approved by the Institution's Animal Review Board.

Antibodies and Reagents

Anti-tubulin, and polyclonal anti-RIP1 were purchased from Santa Cruz; anti-caspase-3 was from Cell Signaling, monoclonal anti-RIP1 was purchased from BD Biosciences. Anti-Beclin 1 was obtained from Stressgen, and anti-LC3 from Novus. Recombinant human Tissue Necrosis Factor (TNF) was purchased from Sigma.

Evans Blue Staining

Fluorescent staining with Evans blue dye (EBD) was used to assess the impairment of sarcolemmal membrane integrity. Six-month-old mice were injected EBD (10 mg/ml in PBS) intraperitoneally with 0.1 ml per 10g body weight. Twenty-four hours later heart tissue was embedded in OCT Tissue Tek (Sakura Finetechnical), and snap-frozen in liquid nitrogen. Seven-μm sections were cut, washed with PBS, and counterstained by phalloidin (Invitrogen). Stained sections were visualized using the fluorescent microscope, and areas of red auto-fluorescence (EBD positive areas) were selected and imaged.

Cell Culture

3T3 fibroblasts were cultured in Dulbecco's modified Eagle's medium supplemented with 10% fetal calf serum and antibiotics (25 U/ml penicillin, 25 μg/ml streptomycin) (Invitrogen) in 5% CO_2 in air at 37 °C. Replication-deficient adenoviruses for CryAB ^{R120G} and Bcl-2 were generated using the AdEasy adenoviral system (Stratagene). Cells were typically infected with adenovirus at a multiplicity of infection of 10 for 2 hours at 37 °C. The cells were then cultured for a further 24 hours in virus-free media before treatment. Cell death was induced with 10 ng/ml of TNF for 10 minutes. For cell death analysis, the Cell Proliferation Kit from Roche was used according to the manufacturer's protocol.

For autophagy assays, rat neonatal cardiomyocytes (RNC) were used. Cells were plated 24 hours before the infection. On the next day, cells were infected with GFP-LC3 adenovirus (provided by J. Sadoshima, University of Medicine and Dentistry of New Jersey), in combination either with AD-CryAB^{R120G}, AD-Bcl-2, or both. Forty-eight hours later, cells were washed, fixed, visualized by fluorescent microscope and analyzed by Image Stream.

Mitochondrial Swelling and Complex I Activity

Mitochondrial swelling experiments were performed as described previously.3 Complex I activity was measured as described.[14] Fifty μg of isolated heart mitochondria were diluted in the reaction mixture consisted of 250 mmol/L sucrose, 1.0 mmol/L EDTA, 50 mmol/L Tris-HCl, pH 7.4, 10 umol/L decylubiquinone (Sigma), and 2 mmol/L KCN. The reaction was initiated by adding 50 μmol/L NADH, and monitored continuously at a wavelength of 272 minus 247 nm at 30 °C for 1 minute. Rotenone (5 μg) was added, and any rotenone-insensitive activity was measured for 1 minute.

ImageStream Data Acquisition and Analysis

This fluorescence image-based method for quantifying LC3 relies on differentiating the-diffuse and punctate forms of LC3 staining. Cells infected with adenovirus carrying GFP-LC3 were co-infected with AD-CryAB^{R120G}, AD-Bcl-2, or both. Forty-eight hours after infection, cells were trypsinized, fixed, excited with a 488 nm laser light and imaged on a time delay integration CCD camera. Images of fixed cells collected on the ImageStream (Amnis), were analyzed using ImageStream Data Exploration and Analysis Software (IDEAS). Because fluorescent probes have broad emission spectra, spectral compensation was digitally performed on a pixel-by-pixel basis prior to data analysis. After compensation, similarity analysis and spot counting was done on in-focus single cell images. Three samples from each group were analyzed using 10,000 cells per sample.

Statistical Analysis

All data are expressed as mean ± S.E. Comparisons between experimental were determined by 1-way or 2-way ANOVA where appropriate, followed by Student's *t*-test. A *P* value of <0.05 was considered statistically significant.

Results

Overexpression of Bcl-2 Increases Lifespan and Ameliorates Cardiac Dysfunction in CryAB^{R120G} Mice

Mice that overexpress Bcl-2 specifically in the cardiomyocytes have been described.[8] We crossed those mice repeatedly into the FVB/N background, the strain in which our other transgenic mice were made, in order to avoid strain specific phenotypes. Cardiomyocyte-restricted Bcl-2 overexpression in an FVB/N background was benign with no effects observed on heart structure or function (data not shown). The Bcl-2 transgene continued to be strongly

expressed in the hearts of the FVB/N strain (Figure 1A) and when it was crossed into the CryAB^{R120G} background as well (Figure 1A), with quantitation of the signals indicating overexpression levels of approximately 5-fold in animals carrying one copy of the Bcl-2 transgene and 9-fold in animals with 2 copies (homozygous for the transgene). We used double transgenic animals that carried 1 copy of each transgene (Bcl-2 and CryAB^{R120G}) for all experiments in order to avoid any effects due to insertional mutagenic events. As shown previously, cardiac-restricted expression of CryAB^{R120G} leads to premature lethality by the age of 7–8 months (Figure 1B) due to HF.[2] Life spans of the CryAB^{R120G}/Bcl-2 mice were significantly increased when compared to the CryAB^{R120G} mice. However, all of these mice also died prematurely with no survivors by 8.5–9 months of age (Figure 1B).

We previously showed that overexpression of CryAB^{R120G} contributes to the LV dysfunction characterized by the progressive transition from concentric hypertrophy to dilated cardiomyopathy at the age of 6 months.[2] In association with their prolonged life span, CryAB^{R120G}/Bcl-2 mice displayed an attenuated cardiac hypertrophic response (Figure 1C). To determine whether overexpression of Bcl-2 was sufficient to attenuate adverse cardiac remodeling in CryAB^{R120G} mice, we examined cardiac structure using standard morphometric analyses and 2D-directed M-mode echocardiography (Figure 1C and Table 1). Figure 1B shows that heart weight-to-body weight ratios of the single CryAB^{R120G} mice at 4 and 6 months were significantly greater than age-matched NTG and CryAB^{R120G}/Bcl-2 mice. In addition, marked disparities in cardiac function between the CryAB^{R120G} and CryAB^{R120G}/Bcl-2 mice were apparent as well (Table 1). At 6 months of age, when the CryAB^{R120G} animals were already in failure, the heart rate and shortening fraction of the CryAB^{R120G}/Bcl-2 mice were conserved with significantly better LV function (Table 1).

Bcl-2 Expression Prevents Mitochondrial Swelling and Blunts the Apoptotic Response in CryAB^{R120G} mice

Constitutive overexpression of mutant CryAB^{R120G} leads to mitochondrial dysfunction, a precocious and lasting 50% reduction in Complex I activity, opening of the mitochondrial permeability transition pore (MPTP) and activation apoptotic cell death.[3] MPTP opening results in mitochondrial swelling and irreversible loss of the matrix and intermembrane content. 8 If this cannot be prevented, the outer mitochondrial membrane will eventually rupture, releasing potent apoptogens into the cytoplasm and triggering apoptotic cell death. Pro-apoptotic members of the Bcl-2 family such as Bax and Bak play important roles in mediating mitochondrial swelling. Since the anti-apoptotic family members, Bcl-2 and Bcl-XL are able to prevent the permeabilization of the outer mitochondrial membrane by directly inhibiting Bax and Bak,15 we first analyzed this potential beneficial effect in the CryAB^{R120G}/Bcl-2 hearts. Mitochondria isolated from 2 month old CryAB^{R120G} mice were extremely sensitive to Ca^{2+}-induced swelling,[3] but the mitochondria derived from the CryAB^{R120G}/Bcl-2 mice were essentially normal (Figure 2A). At the same time, mitochondrial complex I activity in the CryAB^{R120G}/Bcl-2 hearts showed the same deficits apparent in the CryAB^{R120G}-derived material, showing that Bcl-2 overexpression is not able to rescue the respiratory deficits in the CryAB^{R120G} mitochondria (Figure 2B).

To begin to explore the mechanisms responsible for Bcl-2-mediated attenuation of cardiomyocyte apoptosis we evaluated the extent of DNA fragmentation longitudinally in the NTG, CryAB^{R120G} and CryAB^{R120G}/Bcl-2 hearts by quantitating TUNEL-positive nuclei located in identified cardiomyocytes. We observed significant decreases in the number of TUNEL positive nuclei in 2 and 6 month old CryAB^{R120G}/Bcl-2 hearts as compared to CryAB^{R120G} (Figure 2C). We confirmed that we were observing decreases in apoptosis by measuring reduced levels of activated caspase-3 in the CryAB^{R120G}/Bcl-2 but not in CryAB^{R120G} hearts (Figure 2D).

We then measured the release of cytochrome c from mitochondria into the cytosol in the hearts of 5-month-old CryAB^{R120G} and CryAB^{R120G}/Bcl-2 mice. Representative Western blots derived from the mitochondrial and cytosolic proteins showed that in CryAB^{R120G}/Bcl-2 mouse hearts, cytosolic cytochrome c levels were significantly lower than in the CryAB^{R120G} hearts although they remained higher than the level observed in the NTG littermates (Figure 2E).

Protein Aggregation in CryAB^{R120G}/Bcl-2 Mice is Reduced

CryAB^{R120G}-mediated DRM is a protein misfolding disease characterized by accumulation of insoluble protein depositions, whose accumulations can have both toxic[14] and protective functions.[16] Although expression of Bcl-2 in the CryAB^{R120G} hearts did not completely prevent aggregate formation, electron microscopy revealed major disparities in protein deposition architecture. The aggresomes[16,17] in the CryAB^{R120G} hearts appeared to be largely homogenous, consisting of uniformly solid, granulofilamentous bodies, while in the CryAB^{R120G}/Bcl-2 hearts they appeared as heterogeneous masses of small electron-dense material interspersed with mitochondria (Figure 3A). Immunofluorescent staining for CryAB was used to quantitate the cytoplasmic area occupied by the aggresomes (Figure 3B) and confirmed significant decreases in their accumulation at all ages measured (Figure 3C).

Protein aggregates may form by abnormal folding or by disturbance of intracellular protein degradation pathways. While autophagy is known to play a critical role in the major degradation pathways for cellular protein and organelles, it is becoming increasingly apparent that autophagy is an important cellular process that can be activated in response to the accumulation of misfolded proteins.[18] Autophagy is upregulated in rat neonatal cardiomyocytes infected with CryAB^{R120G} adenovirus and blunting autophagy in CryAB^{R120G} hearts accelerated and increased development of the cardiac pathology.[19]

Given those data and the observation that CRYAB^{R120G}/Bcl-2 hearts displayed significant decreases in protein aggregate levels, we wished to evaluate and compare the autophagic response in CryAB^{R120G} and CryAB^{R120G}/Bcl-2 hearts. Beclin 1 is considered to be a key player in autophagy. Beclin 1 promotes autophagic activity[20] and is involved in the recruitment of membranes to form the autophagosome. However, in contrast to our expectation that autophagy would be increased in both the CryAB^{R120G} and CryAB^{R120G}/Bcl-2 hearts, we observed modest but significant reductions in Beclin 1 levels in both the CryAB^{R120G} and CryAB^{R120G}/Bcl-2 hearts relative to NTG (Figure 4A).

Given the complex nature of autophagy, we analyzed additional markers of the process. Formation and maturation of autophagosomes is accompanied by intracellular translocation and processing of microtubule-associated protein 1 light chain 3 (LC3),[21] an important component of the autophagosome membrane and one of the most reliable markers of autophagy. Western Blot analysis showed accumulation of cleaved LC3-II exclusively in the hearts of CryAB^{R120G}/Bcl-2 but not CryAB^{R120G} mice, suggesting a significant augmentation of an autophagic response in the double transgenic mice (Figure 4B).

In order to gain a qualitative assessment of autophagy, we carried out transmission electron microscopy on hearts derived from the single and double transgenic hearts at 5 months. As expected, the CryAB^{R120G} hearts showed the usual pathology at this stage with significant accumulations of large, granulofilamentous aggregates, disrupted mitochondria with massive cristae lysis and sarcomere disruption. However, strikingly, there was a paucity of any structures that could be identified as either intermediates or late stages in the autophagic pathway (Figure 5A). In contrast, the fields from the double transgenic hearts contain numerous intermediates/participants in the autophagic pathway, including amphisomes, the autophagic

vacuoles formed upon fusion between autophagosomes and endosomes, lysosomes and autolysosomes (Figure 5B–D).

To quantitate the increase in autophagic activity in response to Bcl-2 overexpression, neonatal rat cardiomyocytes were infected with GFP-LC3 - autophagy–reporter adenovirus, followed by infection with AD-CryAB^{R120G}, AD-Bcl-2 or a combination of both. Forty-eight hours later cells were fixed, visualized by fluorescent microscope and analyzed using the Image Stream system (Figure 6). LC3 undergoes a significant redistribution during autophagy, changing from a diffused cytosolic signal to punctate dots that mark the mature autophagosome.[22] After 48 hours, the abundance of punctuated LC3 was almost 5-fold higher in the cardiomyocytes infected with both AD-Bcl-2 and AD-CryAB^{R120G} in comparison to AD-CryAB^{R120G} only (Figure 6B). Blockade of autophagosome formation using 3-MA significantly reduced the accumulation of punctuated LC3 in R120G/Bcl-2 infected cardiomyocytes.

Blunting the Apoptotic Response Leads to Necrosis in CryAB^{R120G}/Bcl-2 Mice

Our data showed that overproduction of the anti-apoptotic protein Bcl-2 increased the life span of the CryAB^{R120G} animals, indicating that the intrinsic apoptotic pathway does play a pathogenic role in DRM. However, the animals still die prematurely, so abrogation of apoptosis is clearly not sufficient to rescue the phenotype. Historically, apoptosis has been defined as a type of cell death that is morphologically distinct from other types of cell death such as necrosis.[23] Despite the long held view that necrosis is an accidental and uncontrolled form of cell death, recent studies have revealed that necrosis is probably tightly controlled, and intriguing interactions between the apoptotic and necrotic machinery have been uncovered.[24] Eliminating genes encoding proteins controlling apoptosis resulted in the conversion of an apoptotic phenotype to a necrotic one, both in vitro and in vivo.[25] We hypothesized that by overexpressing Bcl-2 and decreasing apoptotic flux in the absence of not affecting the primary genetic lesion (expression of CryAB^{R120G}); we might have shifted the cell death balance to necrosis.

Evans Blue dye (EBD) analyses were performed in order to detect necrotic cell death-related membrane abnormalities in the myocardium of NTG, CryAB^{R120G} and CryAB^{R120G}/Bcl-2 hearts (Figure 7A). NTG cardiomyocytes were impervious to EBD (not shown). In the hearts from 6 month CryAB^{R120G} mice, which are undergoing extensive apoptotic cell death,[3] sporadic EBD-positive myocytes were observed (Figure 7A). However, the number of EDB-positive cells in CryAB^{R120G}/Bcl-2 hearts were significantly increased (Figure 7A, lower panel and B).

Pharmacological and genetic evidence suggests that necrosis can occur in a tightly regulated manner.[26] Cell death inducers such as TNF promote either apoptosis or necrosis depending on the specific experimental setting.[27] When apoptotic cell death is inhibited by anti-apoptotic factors, a process of programmed necrotic death can occur.[28] Although the proteins regulating necrosis are largely undefined, recent data indicate that some regulatory mechanisms may be shared or intersect with apoptosis,[29] and RIP1 kinase may play an important role in deciding between necrosis and survival when the apoptotic signal is blocked.[29] Consistent with this hypothesis, we found significantly higher RIP1 levels in 6 month old CryAB^{R120G}/Bcl-2 hearts compared to NTG and CryAB^{R120G} samples (Figure 7C and D). Interestingly, CryAB^{R120G} hearts showed markedly reduced RIP1 levels.

We tested the hypothesis that co-expression of Bcl-2 and CryAB^{R120G} is sufficient to cause increased levels of RIP1. 3T3 cells were infected with adeno-CryAB^{R120G} (R group), adeno-Bcl-2 (B group), or with both (RB group) and RIP1 accumulation determined 24 hours later by immunohistochemistry (Online Figure IA). Confirming the hypothesis, RB cells showed

more than a 7-fold accumulation of RIP1 compared to R, B and control cells (Online Figure IB).

We next tested whether accumulation of RIP1 was sufficient to increase the sensitivity of infected 3T3 cells to TNF-mediated necrosis (Online Figure IC). Cells were treated with low levels of TNF (**Materials and Methods**) and the level of cell death was evaluated. While non-transfected, R120G and Bcl-2-infected cells showed only minor responses to TNF, cell death in RB cells increased by 100%, indicating a significantly elevated sensitivity of RB cells to TNF-mediated necrosis. However, when the effect of TNF was analyzed in the presence of necrostatin, a specific inhibitor of RIP1, the sensitizing effect was completely abrogated.

Discussion

Several etiologic factors have been linked to the onset and development of dilated cardiomyopathy and HF in the CryAB^{R120G} mice. These include mitochondrial abnormalities, myofilament disarray, reduction in contractile function due to accumulation of insoluble aggregates, and apoptotic cell loss.[3,14,17,30] Each of these parameters contributes to CryAB^{R120G} cardiac pathogenesis. In this study, we wished to explore the role of apoptosis in the progression of HF in CryAB-mediated DRM and took a genetic approach to inhibit cardiomyocyte apoptosis by driving overexpression of anti-apoptotic Bcl-2 in the hearts of CryAB^{R120G} mice.

There are considerable data suggesting that apoptotic cell death can play an important or even determining role in progressive cardiac remodeling,[31,32] with overexpression of either intrinsic or extrinsic apoptotic pathway components causing dilated cardiomyopathy.[28] Previous studies suggest a beneficial effect for increased Bcl-2 expression in different genetic models of cardiomyopathy, including the desmin nulls, a model of ischemic/reperfusion injury, as well as in CryAB^{R120G} mice with cardiac restricted overexpression of secretable TNF.[10,11,31] We show here that overproduction of Bcl-2 in the heart not only reduces the level of CryAB^{R120G}-induced cardiac apoptosis but also impacts, albeit temporarily, on adverse cardiac remodeling, progressive hypertrophy and decreased fractional shortening. While abrogation of apoptosis slows loss of cardiac function, it does not halt a pathogenic progression that results in eventual dilation and HF.

In addition to clarifying the role of apoptosis in this model, our data provide several new insights into the mechanism of CryAB^{R120G}-mediated pathology. As is the case for most protein conformation-based disease, CryAB^{R120G}-DRM is characterized by the accumulation of abnormal protein aggregates.[2] Autophagy can be involved in the intracellular degradation of aggregation–prone proteins, such as alpha-synuclein and huntingtin,[33,34] and Beclin 1 is one of the key players in autophagosome formation.[35] However, despite the increase in the number of lysosomes and autophagosomes in both CryAB^{R120G} and CryAB^{R120G}/Bcl-2 mice, the level of Beclin 1 was significantly reduced in these models. This is in agreement with studies from other groups showing Beclin 1 reduction in other protein misfolding diseases such as Alzheimer or Huntington.[36] How Beclin 1 is regulated in cardiomyocytes and why it is decreased in the latter stages of the DRM model remains unclear. Overexpression of mutant CryAB^{R120G} itself did not directly result in reduced Beclin 1 levels. However, the BH3 domain of Beclin 1 can bind directly to Bcl-2,[37] with the interaction actually inhibiting autophagy but leaving the anti-apoptotic activity of Bcl-2 intact.[38] In beginning to ask how overexpression of Bcl-2 affects the autophagic status of CryAB^{R120G} mice, we find it intriguing that critical players in the apoptotic and autophagic pathways can interact. Unlike other studies showing the anti-autophagic activity of Bcl-2,[39] the autophagic response remained largely intact as evidenced by increased LC3-II levels and the significant reduction in protein aggregate accumulation.

Activation of autophagy under conditions of inhibited apoptotic cell death has been previously documented in Bak/Bax knockout mice.[40]

The precise role of autophagy in the progression of HF remains unclear. In some HF models, amplification of the autophagic response led to pathologic hypertrophy, decreased cardiac performance, and promotion of autophagic cell death.[41] In other studies, autophagy protected the heart by scavenging and eliminating misfolded proteins.[42] It appears that autophagy can lead to different outcomes depending upon disease context and severity. Future studies using genetic approaches are underway to define the exact role of autophagy in our model at the different disease stages.

Necrosis has been often viewed as an accidental and unregulated event but data are now rapidly accumulating that suggest necrosis can also be thought of as programmed cell death.[43] The cell death program, whether by apoptosis or by necrosis, is mediated through an integrated cascade, which can be assessed at multiple junction sites and propagated through numerous branch points.[29] Recent studies point to RIP1 as a possible “molecular switch” that can determine whether the cell succumbs through apoptosis or necrosis.[44] In our model, overproduction of Bcl-2 led to increased RIP1 with a concomitant increase in necrosis and these admittedly preliminary but intriguing data point the way for further exploration of whether these markers are general or more specific to different but related cell death processes.

That overexpression of Bcl-2 leads to a reversal of calcium sensitivity of the mitochondria and may lead to a switch from apoptosis to autophagy and necrosis argues strongly for the existence of complex regulatory interactions between these scavenger/cell death mechanisms and could explain the limited success of anti-apoptotic therapies. An additional complication is the different roles these processes could play at different times in disease progression and presentation. Although considerable work will be required to explain the observations outlined in this manuscript, an appreciation of the complexities and understanding the underlying molecular pathways will help define effective combinational therapies.

Novelty and Significance

What is Known?

- Mutations in αB-crystallin can cause a dilated cardiomyopathy and heart failure.
- Although apoptotic cell death contributes to the development of cardiac pathology, its necessity and sufficiency in the cardiac pathogenesis is not known.

What New Information Does This Article Contribute?

- In vivo evidence that death pathways other than apoptosis are capable of causing cardiomyopathy and heart failure in this animal model
- First demonstration in this animal model that abrogating the intrinsic pathway of apoptosis in the heart is possible and that, while life is prolonged, the animal still dies prematurely
- Indirectly supports a model for the interlinking of different death pathways in the pathogenic process that leads to cardiac death.

The missense R120G mutation in the small heat shock protein alpha-B-crystallin (CryABR120G) causes a desmin-related myopathy (DRM). This skeletal and cardiac disease is characterized by the formation of desmin- and CryAB-containing aggregates within muscle fibers, including those within the heart. Mice with cardiac-specific overexpression of CryABR120G develop severe cardiomyopathy at 3 months of age and

die at 6–7 months from heart failure. Previous studies showed that overexpression of CryABR120G results in formation of perinuclear aggresomes, and accumulation of pre-amyloid oligomer (PAO). PAO is considered to be the cytotoxic entity in many of protein misfolding-based diseases and we noted extensive apoptosis in these hearts. Because of this, we asked whether we could impact materially on disease progression by interfering with apoptosis and so, we crossed the CryABR120G mice with a mouse that specifically expressed the anti-apoptotic molecule, Bcl-2, in cardiomyocytes. To our surprise, while apoptosis was largely ameliorated, the mice still died although they lived 20% longer than mice that did not express increased levels of Bcl-2. In order to understand the cause of death, we explored whether other death pathways were activated and found that, indeed, while apoptosis was shut down, necrosis was activated. These findings have implications for using the death pathways as therapeutic targets and indicate that multiple pathway interactions will need to be considered and tested for any potential therapeutics aimed at a single pathway.

Supplementary Material

Refer to Web version on PubMed Central for supplementary material.

Acknowledgments

Sources of Funding

This work was supported by National Institutes of Health grants P01HL69799, P50HL074728, P50HL077101, P01HL059408, R01HL087862 (J.R.)

Abbreviations

HF	heart failure
CryAB	αB-crystallin
EBD	Evans Blue Dye
RNC	rat neonatal cardiomyocytes
MPTP	Mitochondrial Permeability Transition Pore
RIP1	Receptor Interacting Protein 1
TNF	Tumor Necrosis Factor
TG	transgenic
NTG	non-transgenic

References

1. Vicart P, Caron A, Guicheney P, Li Z, Prevost MC, Faure A, Chateau D, Chapon F, Tome F, Dupret JM, Paulin D, Fardeau M. A missense mutation in the alphaB-crystallin chaperone gene causes a desmin-related myopathy. Nat Genet 1998;20:92–95. [PubMed: 9731540]
2. Wang X, Osinska H, Klevitsky R, Gerdes AM, Nieman M, Lorenz J, Hewett T, Robbins J. Expression of R120G-alphaB-crystallin causes aberrant desmin and alphaB-crystallin aggregation and cardiomyopathy in mice. Circ Res 2001;89:84–91. [PubMed: 11440982]
3. Maloyan A, Sanbe A, Osinska H, Westfall M, Robinson D, Imahashi K, Murphy E, Robbins J. Mitochondrial dysfunction and apoptosis underlie the pathogenic process in alpha-B-crystallin desmin-related cardiomyopathy. Circulation 2005;112:3451–3461. [PubMed: 16316967]

4. Foo RS, Mani K, Kitsis RN. Death begets failure in the heart. J Clin Invest 2005;115:565–571. [PubMed: 15765138]

5. Kirshenbaum LA, de Moissac D. The bcl-2 gene product prevents programmed cell death of ventricular myocytes. Circulation 1997;96:1580–1585. [PubMed: 9315550]

6. Garland JM, Halestrap A. Energy metabolism during apoptosis. Bcl-2 promotes survival in hematopoietic cells induced to apoptose by growth factor withdrawal by stabilizing a form of metabolic arrest. J Biol Chem 1997;272:4680–4688. [PubMed: 9030519]

7. Kroemer G, Galluzzi L, Brenner C. Mitochondrial membrane permeabilization in cell death. Physiol Rev 2007;87:99–163. [PubMed: 17237344]

8. Green DR, Kroemer G. The pathophysiology of mitochondrial cell death. Science 2004;305:626–629. [PubMed: 15286356]

9. Chen Z, Chua CC, Ho YS, Hamdy RC, Chua BH. Overexpression of Bcl-2 attenuates apoptosis and protects against myocardial I/R injury in transgenic mice. Am J Physiol Heart Circ Physiol 2001;280:H2313–2320. [PubMed: 11299236]

10. Imahashi K, Schneider MD, Steenbergen C, Murphy E. Transgenic expression of Bcl-2 modulates energy metabolism, prevents cytosolic acidification during ischemia, and reduces ischemia/reperfusion injury. Circ Res 2004;95:734–741. [PubMed: 15345651]

11. Weisleder N, Taffet GE, Capetanaki Y. Bcl-2 overexpression corrects mitochondrial defects and ameliorates inherited desmin null cardiomyopathy. Proc Natl Acad Sci U S A 2004;101:769–774. [PubMed: 14715896]

12. Pinton P, Ferrari D, Magalhaes P, Schulze-Osthoff K, Di Virgilio F, Pozzan T, Rizzuto R. Reduced loading of intracellular Ca(2+) stores and downregulation of capacitative Ca(2+) influx in Bcl-2-overexpressing cells. J Cell Biol 2000;148:857–862. [PubMed: 10704437]

13. Foyouzi-Youssefi R, Arnaudeau S, Borner C, Kelley WL, Tschopp J, Lew DP, Demaurex N, Krause KH. Bcl-2 decreases the free Ca2+ concentration within the endoplasmic reticulum. Proc Natl Acad Sci U S A 2000;97:5723–5728. [PubMed: 10823933]

14. Maloyan A, Osinska H, Lammerding J, Lee RT, Cingolani OH, Kass DA, Lorenz JN, Robbins J. Biochemical and mechanical dysfunction in a mouse model of desmin-related myopathy. Circ Res 2009;104:1021–1028. [PubMed: 19299643]

15. Youle RJ, Strasser A. The BCL-2 protein family: opposing activities that mediate cell death. Nat Rev Mol Cell Biol 2008;9:47–59. [PubMed: 18097445]

16. Sanbe A, Osinska H, Villa C, Gulick J, Klevitsky R, Glabe CG, Kayed R, Robbins J. Reversal of amyloid-induced heart disease in desmin-related cardiomyopathy. Proc Natl Acad Sci U S A 2005;102:13592–13597. [PubMed: 16155124]

17. Sanbe A, Osinska H, Saffitz JE, Glabe CG, Kayed R, Maloyan A, Robbins J. Desmin-related cardiomyopathy in transgenic mice: a cardiac amyloidosis. Proc Natl Acad Sci U S A 2004;101:10132–10136. [PubMed: 15220483]

18. Levine B, Kroemer G. Autophagy in the pathogenesis of disease. Cell 2008;132:27–42. [PubMed: 18191218]

19. Tannous P, Zhu H, Johnstone JL, Shelton JM, Rajasekaran NS, Benjamin IJ, Nguyen L, Gerard RD, Levine B, Rothermel BA, Hill JA. Autophagy is an adaptive response in desmin-related cardiomyopathy. Proc Natl Acad Sci U S A 2008;105:9745–9750. [PubMed: 18621691]

20. Zeng X, Overmeyer JH, Maltese WA. Functional specificity of the mammalian Beclin-Vps34 PI 3-kinase complex in macroautophagy versus endocytosis and lysosomal enzyme trafficking. J Cell Sci 2006;119:259–270. [PubMed: 16390869]

21. Zakeri Z, Melendez A, Lockshin RA. Detection of autophagy in cell death. Methods Enzymol 2008;442:289–306. [PubMed: 18662576]

22. Kabeya Y, Mizushima N, Ueno T, Yamamoto A, Kirisako T, Noda T, Kominami E, Ohsumi Y, Yoshimori T. LC3, a mammalian homologue of yeast Apg8p, is localized in autophagosome membranes after processing. Embo J 2000;19:5720–5728. [PubMed: 11060023]

23. Kroemer G, Galluzzi L, Vandenabeele P, Abrams J, Alnemri ES, Baehrecke EH, Blagosklonny MV, El-Deiry WS, Golstein P, Green DR, Hengartner M, Knight RA, Kumar S, Lipton SA, Malorni W, Nunez G, Peter ME, Tschopp J, Yuan J, Piacentini M, Zhivotovsky B, Melino G. Classification of

cell death: recommendations of the Nomenclature Committee on Cell Death 2009. Cell Death Differ 2009;16:3–11. [PubMed: 18846107]

24. Vanlangenakker N, Berghe TV, Krysko DV, Festjens N, Vandenabeele P. Molecular mechanisms and pathophysiology of necrotic cell death. Curr Mol Med 2008;8:207–220. [PubMed: 18473820]
25. Galluzzi L, Maiuri MC, Vitale I, Zischka H, Castedo M, Zitvogel L, Kroemer G. Cell death modalities: classification and pathophysiological implications. Cell Death Differ 2007;14:1237–1243. [PubMed: 17431418]
26. Golstein P, Kroemer G. A multiplicity of cell death pathways. Symposium on apoptotic and non-apoptotic cell death pathways. EMBO Rep 2007;8:829–833. [PubMed: 17721445]
27. Hehlgans T, Pfeffer K. The intriguing biology of the tumour necrosis factor/tumour necrosis factor receptor superfamily: players, rules and the games. Immunology 2005;115:1–20. [PubMed: 15819693]
28. Degterev A, Yuan J. Expansion and evolution of cell death programmes. Nat Rev Mol Cell Biol 2008;9:378–390. [PubMed: 18414491]
29. Hitomi J, Christofferson DE, Ng A, Yao J, Degterev A, Xavier RJ, Yuan J. Identification of a molecular signaling network that regulates a cellular necrotic cell death pathway. Cell 2008;135:1311–1323. [PubMed: 19109899]
30. Maloyan A, Gulick J, Glabe CG, Kayed R, Robbins J. Exercise reverses preamyloid oligomer and prolongs survival in alphaB-crystallin-based desmin-related cardiomyopathy. Proc Natl Acad Sci U S A 2007;104:5995–6000. [PubMed: 17389375]
31. Haudek SB, Taffet GE, Schneider MD, Mann DL. TNF provokes cardiomyocyte apoptosis and cardiac remodeling through activation of multiple cell death pathways. J Clin Invest 2007;117:2692–2701. [PubMed: 17694177]
32. Wencker D, Chandra M, Nguyen K, Miao W, Garantziotis S, Factor SM, Shirani J, Armstrong RC, Kitsis RN. A mechanistic role for cardiac myocyte apoptosis in heart failure. J Clin Invest 2003;111:1497–1504. [PubMed: 12750399]
33. Ravikumar B, Sarkar S, Rubinsztein DC. Clearance of mutant aggregate-prone proteins by autophagy. Methods Mol Biol 2008;445:195–211. [PubMed: 18425452]
34. Webb JL, Ravikumar B, Atkins J, Skepper JN, Rubinsztein DC. Alpha-Synuclein is degraded by both autophagy and the proteasome. J Biol Chem 2003;278:25009–25013. [PubMed: 12719433]
35. Liang XH, Jackson S, Seaman M, Brown K, Kempkes B, Hibshoosh H, Levine B. Induction of autophagy and inhibition of tumorigenesis by beclin 1. Nature 1999;402:672–676. [PubMed: 10604474]
36. Pickford F, Masliah E, Britschgi M, Lucin K, Narasimhan R, Jaeger PA, Small S, Spencer B, Rockenstein E, Levine B, Wyss-Coray T. The autophagy-related protein beclin 1 shows reduced expression in early Alzheimer disease and regulates amyloid beta accumulation in mice. J Clin Invest 2008;118:2190–2199. [PubMed: 18497889]
37. Oberstein A, Jeffrey PD, Shi Y. Crystal structure of the Bcl-XL-Beclin 1 peptide complex: Beclin 1 is a novel BH3-only protein. J Biol Chem 2007;282:13123–13132. [PubMed: 17337444]
38. Ciechomska IA, Goemans GC, Skepper JN, Tolkovsky AM. Bcl-2 complexed with Beclin-1 maintains full anti-apoptotic function. Oncogene 2009;28:2128–2141. [PubMed: 19347031]
39. Pattingre S, Tassa A, Qu X, Garuti R, Liang XH, Mizushima N, Packer M, Schneider MD, Levine B. Bcl-2 antiapoptotic proteins inhibit Beclin 1-dependent autophagy. Cell 2005;122:927–939. [PubMed: 16179260]
40. Shimizu S, Kanaseki T, Mizushima N, Mizuta T, Arakawa-Kobayashi S, Thompson CB, Tsujimoto Y. Role of Bcl-2 family proteins in a non-apoptotic programmed cell death dependent on autophagy genes. Nat Cell Biol 2004;6:1221–1228. [PubMed: 15558033]
41. Zhu H, Tannous P, Johnstone JL, Kong Y, Shelton JM, Richardson JA, Le V, Levine B, Rothermel BA, Hill JA. Cardiac autophagy is a maladaptive response to hemodynamic stress. J Clin Invest 2007;117:1782–1793. [PubMed: 17607355]
42. Matsui Y, Takagi H, Qu X, Abdellatif M, Sakoda H, Asano T, Levine B, Sadoshima J. Distinct roles of autophagy in the heart during ischemia and reperfusion: roles of AMP-activated protein kinase and Beclin 1 in mediating autophagy. Circ Res 2007;100:914–922. [PubMed: 17332429]

43. Galluzzi L, Kroemer G. Necroptosis: a specialized pathway of programmed necrosis. Cell 2008;135:1161–1163. [PubMed: 19109884]

44. Galluzzi L, Kepp O, Kroemer G. RIP Kinases Initiate Programmed Necrosis. J Mol Cell Biol. 2009

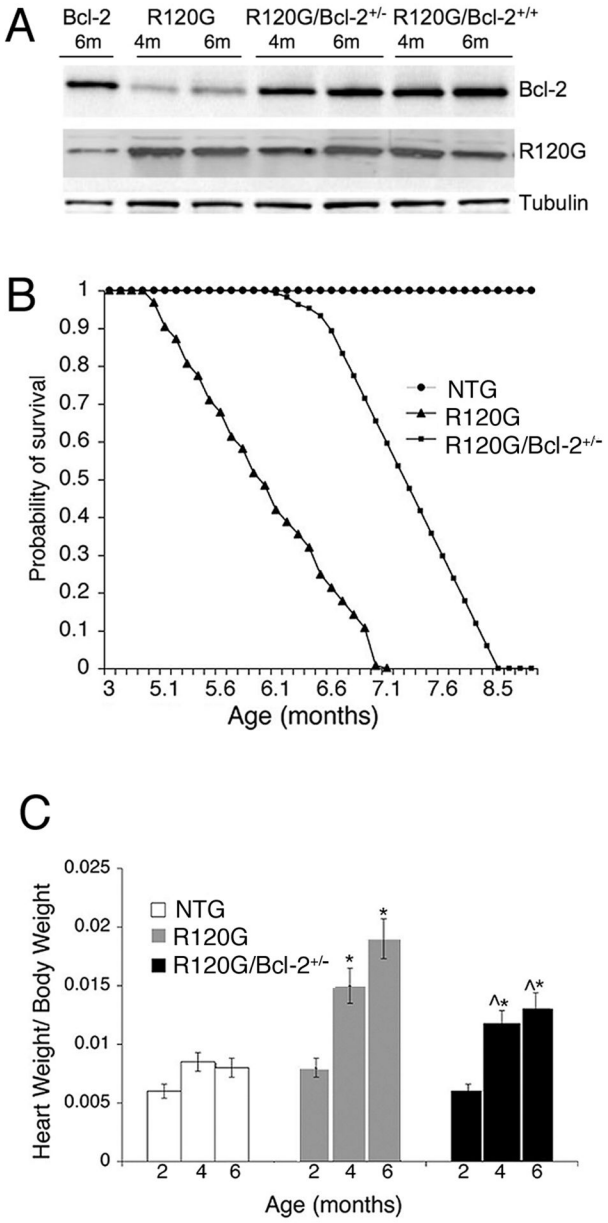

Figure 1.

A, Western blots showing expression levels in the single and double transgenic mice. When placed in the FVB/N background, the Bcl-2 transgene drove expression levels of between 5- (heterozygote) and 10-fold (homozygote, that is, two copies of the transgene) greater than present in NTG mice, with those levels maintained throughout the adult states (4 months and 6 month levels are shown). Placement of the Bcl-2 transgene in the CryAB^{R120G} background did not affect expression of either CryAB or Bcl-2. B, Kaplan-Meier curves for NTG, CryAB^{R120G}, and CryAB^{R120G}/Bcl-2 mice. C, Cardiac hypertrophy from 2 to 6 months in CryAB^{R120G}/Bcl-2 mice compared to CryAB^{R120G}. *P<0.05 versus NTG; ^P<0.05 CryAB^{R120G}.

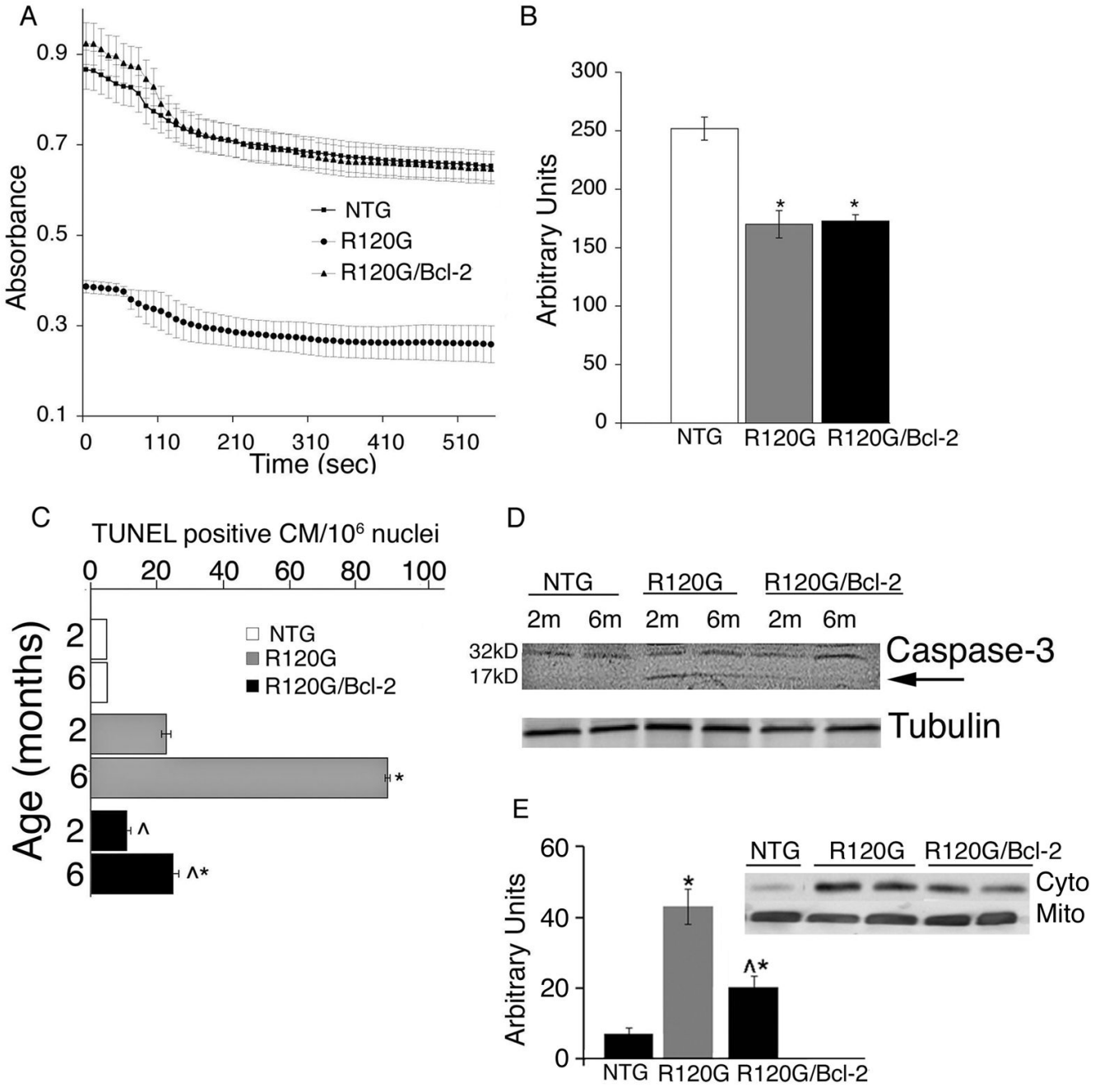

Figure 2.

A, Ca^{2+}-induced swelling of mitochondria from NTG, CryAB^{R120G} and CryAB^{R120G}/Bcl-2 hearts. Mitochondria from 2 month old CryAB^{R120G} hearts were noticeably swollen while mitochondria derived from NTG and CryAB^{R120G}/Bcl-2 hearts appeared normal. B, Complex I activity in 2 month old NTG, CryAB^{R120G}, and CryAB^{R120G}/Bcl-2 hearts. C, Quantification of TUNEL-positive cells in NTG, CryAB^{R120G}, and CryAB^{R120G}/Bcl-2 hearts at 2 and 6 months of age CM; cardiomyocytes. D, activation of caspase-3 (17 kD form, arrow) in TG, but not in CryAB^{R120G}/Bcl-2 hearts; E, The release of cytochrome c from mitochondria to the cytosol was determined by Western blotting in 5-month-old littermate NTG, CryAB^{R120G}, and

CryAB^{R120G}/Bcl-2 hearts. Shown are representative Western blots next to the group data for cytoplasmic cytochrome c levels normalized to tubulin (not shown).

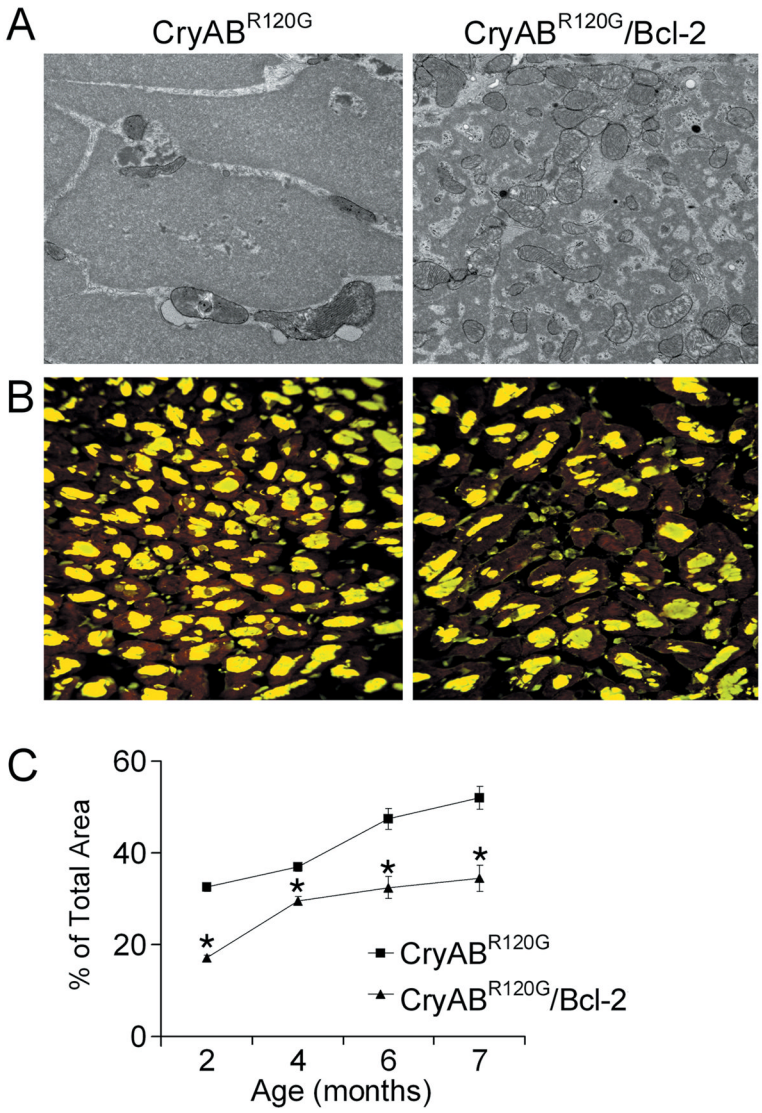

Figure 3.

Overexpression of Bcl-2 significantly reduced the accumulation of misfolded proteins in CryAB^{R120G} hearts. A, Electron microscopy images of protein aggregates from 5-month-old CryAB^{R120G} and CryAB^{R120G}/Bcl-2 hearts. B, Immunofluorescence staining for CryAB (green) with troponin I counterstaining (red) shows decreased aggregate levels. C, Time-dependent quantification of CryAB aggregates using MetaMorph software shows a decreased slope for aggregate accumulation in CryAB^{R120G}/Bcl-2 hearts. *P<0.05 versus CryAB^{R120G}.

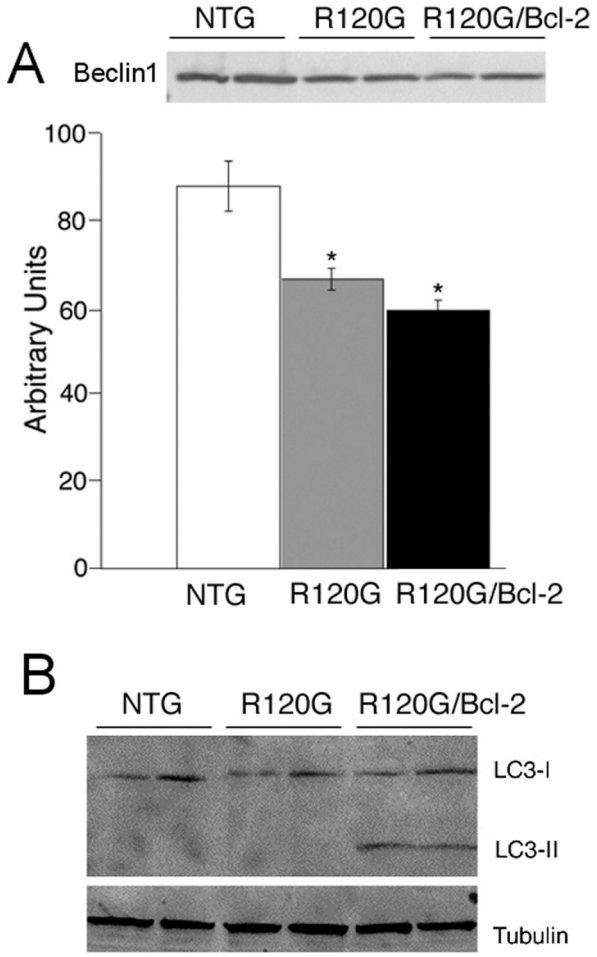

Figure 4.

Autophagy in CryAB^{R120G} and CryAB^{R120G}/Bcl-2 mice. A, Representative Western Blot images and quantification for Beclin 1 in 6-month-old CryAB^{R120G} and CryAB^{R120G}/Bcl-2 hearts. B, Appearance of LC3II as a marker of autophagy. Western Blots were probed with anti-LC3 antibody. Tubulin was used as a loading control, n=4.

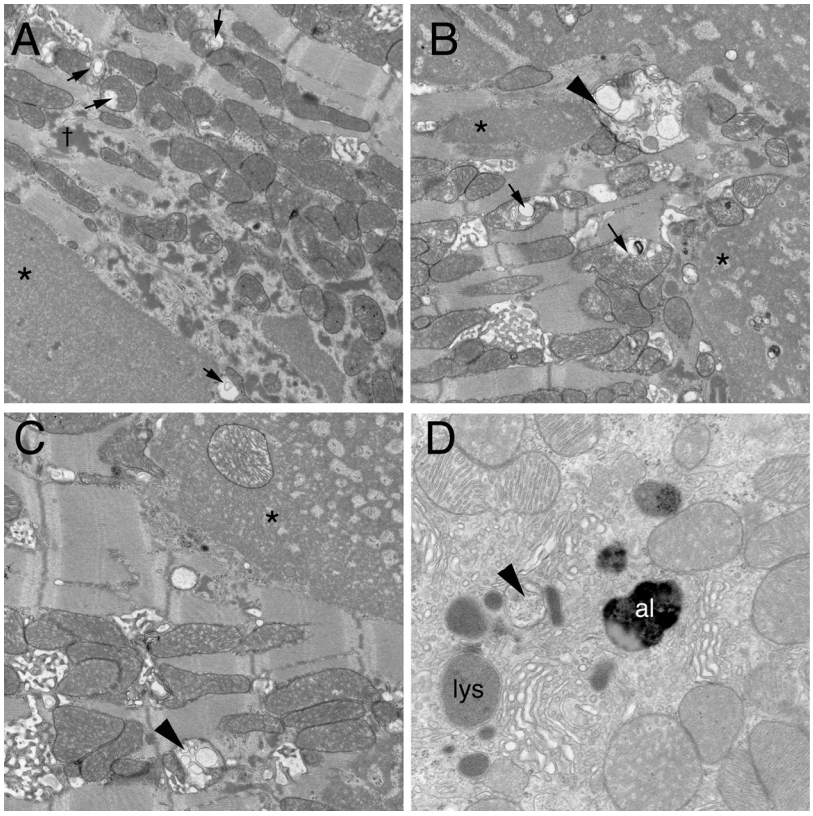

Figure 5.

EM analyses of CryAB^{R120G} and CryAB^{R120G}/Bcl-2 transgenic hearts. Heart were harvested at 5 months and subjected to TEM analyses. Fields were randomly selected from multiple samples from each experimental cohort and viewed at 20,000× or 40,000× (panel D) magnification. A, Typical morphology observed in a 5 month, CryAB^{R120G} ventricle midwall. Type 1 (*) and Type 2 (†) aggregates and the frequent abnormal mitochondria showing cristae lysis and abnormal internal membrane whorls (arrows) are readily apparent.[12] B-D, Three fields from sections derived from the CryAB^{R120G}/Bcl-2 transgenic hearts. Amphisomes (arrowheads), autolysosomes (al) and lysosomes (ly) were invariably present.

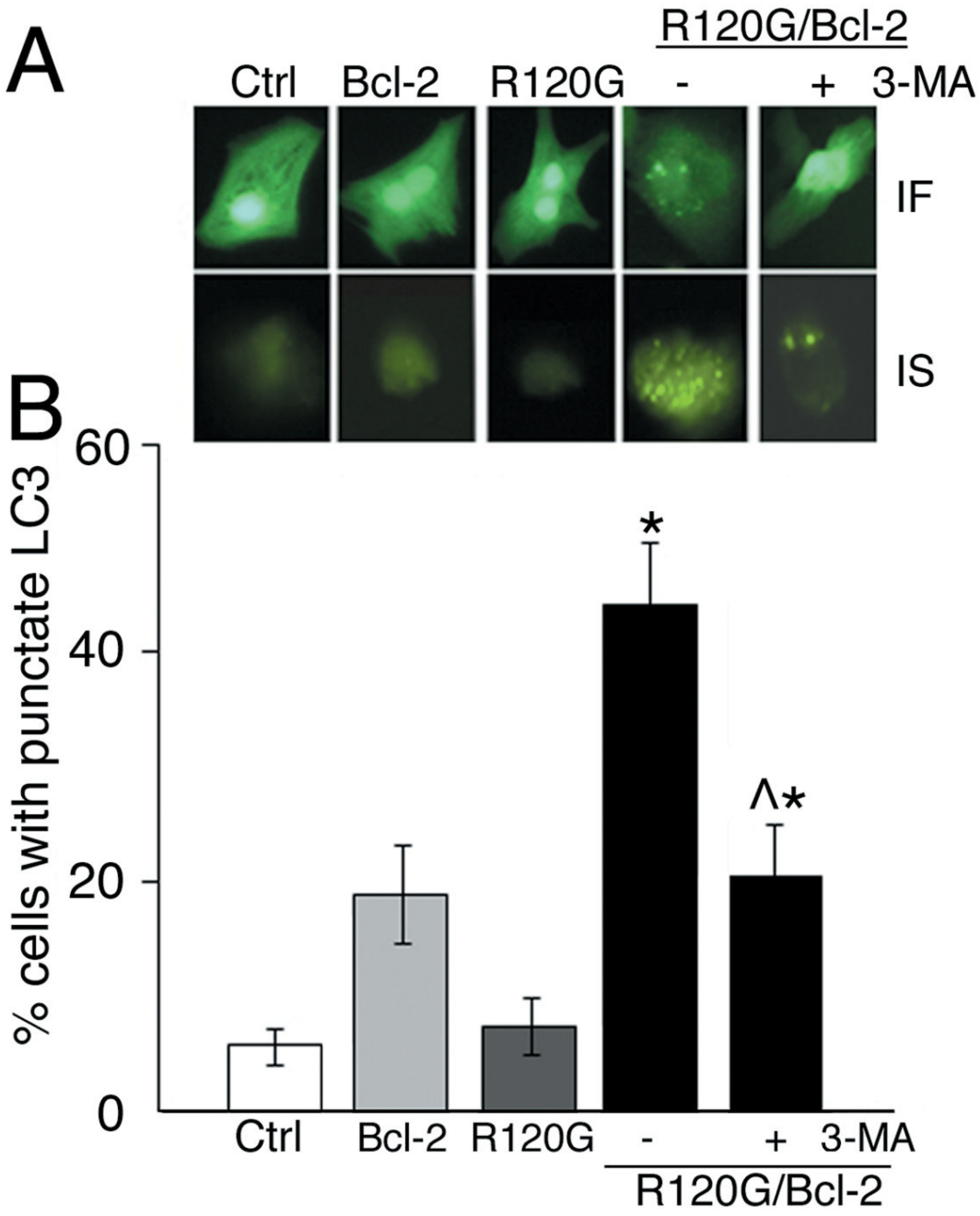

Figure 6.

Immunofluorescence (IF) for GFP-LC3 and ImageStream (IS) analyses of autophagic activity. A, Representative images of individual infected cells obtained using fluorescent microscope and the ImageStream cytometer. Rat neonatal cardiomyocytes expressing GFP-tagged LC3 only (Control; Ctrl) or in combination with Bcl-2, CryAB^{R120G} (R120G) as well as R120G and Bcl-2 (R120G/Bcl-2) together in the absence and presence of 10 μM 3-MA. B, quantification of % of cells with punctate LC3 using IDEAS software. For each cell, the punctate LC3 was differentiated from the diffused signal and the number of spots calculated. *P<0.005 versus NTG, *^P<0.005 versus CryAB^{R120G}.

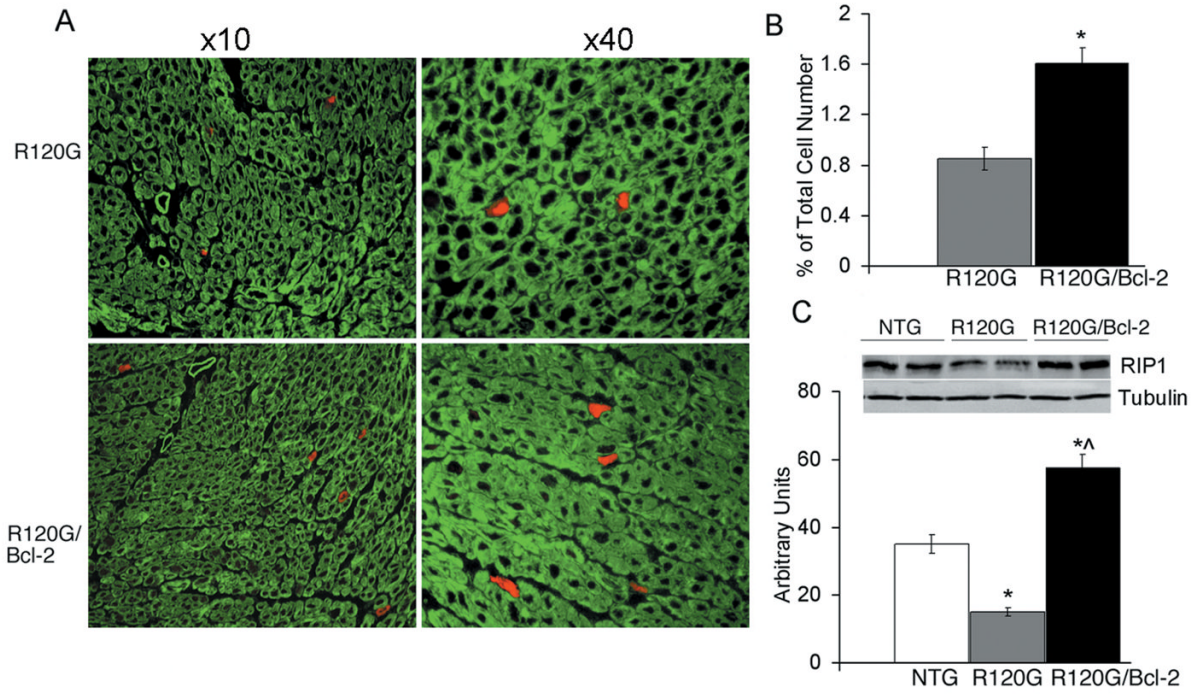

Figure 7.

A, Evans blue permeability of cardiomyocytes derived from CryAB^{R120G} and CryAB^{R120G}/Bcl-2 hearts. Sections were counterstained with phalloidin (green) and visualized by fluorescent microscopy at magnifications of ×10 and ×40. B, Quantification of EBD-positive cells. *P<0.005 versus CryAB^{R120G}. C, Protein derived from CryAB^{R120G} and CryAB^{R120G}/Bcl-2 hearts were electrophoresed in SDS-PAGE, Western blotted and probed with anti-RIP1 and anti-tubulin antibodies. D, Quantification of RIP1 levels using ImageJ software, *P<0.005 versus NTG, ^P<0.005 versus CryAB^{R120G}.

Table 1

Echocardiography and Tissue Doppler measurements

	NTG	CryAB^{R120G}	CryAB^{R120G}/Bcl-2
IVSD	0.079±0.005	0.115±0.004*	0.142±0.04*
IVSs	0.13±0.01	0.18±0.01*	0.12±0.006^
LVIDd	0.365±0.007	0.387±0.014	0.354±0.007
LVPWd	0.105±0.002	0.119±0.004*	0.117±0.002*
FS	41.21±1.14	31.7±1.5*	37.15±1.36^
HR	432±24.89	306.16±19.87*	380.62±17.9^
Septal Aa (mm/sec)	15.66±3.2	4.5±0.3*	8.02±1.8*
Septal Ea/Aa	2.43±0.5	3.11±0.4*	3.3±0.6
Lateral Ea (mm/sec)	26.2±2.2	12.71±2.0*	20.32±2.6^
Lateral Aa (mm/sec)	12.84±1.7	7.44±1.8*	8.45±1.8

Echocardiography and tissue Doppler measurements of NTG, CryAB^{R120G}, and CryAB^{R120G}/Bcl-2 mice. IVSD indicates interventricular septal thickness during diastole; IVSs, interventricular septal thickness during systole; LVIDd, LV internal dimension during diastole; LVPWd, posterior wall thickness during diastole; FS, % fractional shortening; HR, heart rate. Aa, late diastolic myocardial velocity, Ea, early diastolic myocardial velocity.

* $P<0.05$ versus NTG;

^ $P<0.05$ versus CryAB^{R120G}.